HHS Public Access

Author manuscript

*J Vasc Interv Radiol*. Author manuscript; available in PMC 2021 September 01.

Published in final edited form as:

*J Vasc Interv Radiol*. 2020 September ; 31(9): 1483–1491. doi:10.1016/j.jvir.2020.04.038.

# Bariatric Arterial Embolization with Calibrated Radiopaque Microspheres and an Anti-reflux Catheter Suppresses Weight Gain and Appetite-stimulating Hormones in Swine

**Clifford R Weiss, MD, FSIR**[1,*], **Yingli Fu, PhD**[1,*], **Cyrus Beh, PhD**[2], **Charles Hu, PhD**[3], **Dorota Kedziorek, MD**[1], **Eun-Ji Shin, MD**[4], **Robert A Anders, MD**[5], **Aravind Arepally, MD, FSIR**[6], **Dara L Kraitchman, VMD, PhD, FACC**[1]

[1]Russell H Morgan Department of Radiology and Radiological Science, Johns Hopkins University School of Medicine, Baltimore, MD, USA

[2]Biomedical Engineering Department, Johns Hopkins University, Baltimore, MD, USA

[3]Material Science and Engineering, Johns Hopkins University, Baltimore, MD, USA

[4]Department of Gastroenterology, Johns Hopkins University School of Medicine, Baltimore, MD, USA

[5]Department of Pathology, Johns Hopkins University School of Medicine, Baltimore, MD, USA

[6]Department of Radiology, Piedmont Healthcare, Atlanta, GA, USA

## Abstract

**Purpose:** To examine the safety and efficacy of bariatric arterial embolization (BAE) with X-ray-visible embolic microspheres (XEMs) and an anti-reflux catheter in swine.

**Material and Methods:** BAE with selective infusion of XEMs (n = 6) or saline (n = 4, control) into the gastric fundal arteries was performed under X-ray guidance. Weight and plasma hormone levels were measured at baseline and weekly for four weeks after embolization. Cone beam CT (CBCT) images were acquired immediately after embolization and weekly for four weeks. Hormone-expressing cells in the stomach were assessed by immunohistochemical staining.

**Results:** BAE pigs lost weight at one week after embolization followed by significantly impaired weight gain relative to controls (14.3% vs 20.9% at 4 weeks, P = 0.03). Plasma ghrelin levels were significantly lower in embolized animals than those in controls (1221.6 vs 1706.2 at 4 weeks, P <

**Address for correspondence:** Clifford R Weiss, Russell H. Morgan Department of Radiology and Radiological Science, Division of Interventional Radiology, The Johns Hopkins Hospital, 1800 Orleans Street, Sheikh Zayed Tower, Suite 7203, Baltimore, MD 21287, Phone: 443-287-2916, Fax: 410-614-1043, cweiss@jhmi.edu.

*Yingli Fu and Clifford R Weiss contributed equally to this article.



Conflict of Interest:

CRW is a consultant for BTG/Boston Scientific and Medtronic. AA is a founder of Surefire Medical, Inc. Surefire Medical provided devices for the animal studies. All other authors report no conflict of interest

This work was presented as abstracts at the 2014, 2015, and 2016 SIR Annual Scientific Meeting.

0.01). XEMs were visible on X-ray and CBCT during embolization and their radiopacity persisted over four weeks (165.5 HU at week-1 vs. 158.5 HU at week-4, P = 0.9). Superficial mucosal ulcerations were noted in 1 of 6 BAE animals. Ghrelin-expressing cell counts were significantly lower in the gastric fundus (17.7 vs 36.8, P < 0.00001) and antrum (24.2 vs 46.3, P < 0.0001) than those in controls. Gastrin-expressing cell counts were markedly reduced in BAE pigs relative to controls (98.5 vs 127.0, P < 0.02). Trichrome staining demonstrated significantly more fibrosis in BAE animals compared with controls (13.8% vs 8.7%, P < 0.0001).

**Conclusion:** XEMs enabled direct visualization of the embolic material during and after embolization. BAE with XEMs and anti-reflux microcatheters was safe and effective.

### Keywords

Bariatric Arterial Embolization; Radiopaque; X-ray Guidance; Cone Beam CT; Obesity; Ghrelin

## Introduction:

Bariatric arterial embolization (BAE) has recently emerged as a minimally invasive, percutaneous alternative for the treatment of morbid obesity (1–6). This procedure involves transcatheter occlusion of the arteries supplying the gastric fundus, which contains the majority of ghrelin-producing cells (7). A retrospective analysis of patients who have undergone left gastric artery embolization, which provides the dominant blood flow to the gastric fundus, to control upper gastrointestinal bleeding revealed significantly more weight loss post-procedurally than those who underwent embolization of other arteries (8). Preclinical studies have also demonstrated a sustained reduction in weight gain in swine and dogs at four to 16 weeks after BAE (9–11), along with reduced systemic ghrelin levels (11, 12), and reduced density of ghrelin-producing cells in the gastric fundus without significant mucosal damage (13). With these promising results, BAE with particle embolics was quickly translated into the clinic (1–5). However, 40–100% of animals who underwent BAE developed gastric ulcerations irrespective of the size of the embolics used (9, 13–16). Some ulcers appeared away from the embolized fundus, suggesting non-target embolization (NTE) might occur. Because previous BAE studies used radiolucent embolics, none of them could directly assess NTE during delivery.

Given the complex vascular anatomy of the stomach and, in particular, the multiple vessels supplying the gastric fundus (Fig 1A), imaging-visible embolic microspheres in combination with an anti-reflux catheter could allow controlled delivery of the embolic to the target arteries to minimize NTE and enhance safety. In addition, a recent study demonstrated that smaller size embolics were more effective in reducing fundal ghrelin production and weight gain (9). Thus, the purpose of this study is to evaluate the safety and embolization efficacy of BAE with small, uniform (~50-μm) radiopaque embolics (XEMs) and anti-reflux catheters in a large swine model.

## Materials and Methods:

### Embolic Microsphere Synthesis

XEMs were synthesized using custom microfluidic devices with pressure-controlled flow rate to ensure uniform size embolics production. The two-layer polydimethylsiloxane device was fabricated as previously described (17). To prepare XEMs, barium sulfate ($BaSO_4$) suspended in phosphate buffered saline (PBS) was sonicated for 15 minutes, followed by mixing with alginate (FMC polymer, PA) to yield a solution of 10% BaSO4 in 1% alginate. The $BaSO_4$-alginate solution, calcified oleic acid (Sigma-Aldrich, St Louis, MO), and calcium chloride (7%) solution were then introduced in separate channels of the device. The XEMs were generated by side shearing the extruded barium-alginate from the pseudo-check valve into the calcified oil where crosslinking was initiated. The resultant XEMs were stored at room temperature in PBS. Supernatant was analyzed to ensure embolic sterility using an endotoxin assay (Charles River, Wilmington, MA) immediately prior to use.

### Bariatric Arterial Embolization

All animal studies were approved by the Institutional Animal Care and Use Committee. Ten healthy, growing, juvenile Yorkshire swine (28.9 ± 3.9 kg) were randomized to undergo either BAE with XEMs (50-μm, n = 6) or a sham procedure with saline (n = 4) under X-ray guidance. All swine received daily oral omeprazole (40 mg) from three days prior to the procedure to the end of the study except for procedure day when animals received 40 mg intravenous pantoprazole.

Fasted pigs were sedated with a combination of tiletamine (2 mg/kg), zolazepam (2 mg/kg), ketamine (1 mg/kg), and xylazine (2 mg/kg) intramuscularly, and anesthesia was induced with intravenous propofol (~4 mg/kg). Animals were then intubated and mechanically ventilated. General anesthesia was maintained with isoflurane.

BAE and sham procedures were performed by an experienced interventional radiologist (14 years of experience) as previously described (9). Briefly, percutaneous femoral arterial access was obtained under US guidance (Zonare Medical Systems, Mountain View, CA) to advance a guide catheter to the celiac access where digital subtraction angiograms (DSAs) were acquired to map the gastric vasculature. Each fundal branch was then catheterized with an anti-reflux microcatheter (Surefire MT®, Surefire) and steerable 0.016 Fathom guidewire (Boston Scientific). In swine undergoing BAE, DSA was obtained during injection of ~0.5 ml of XEMs suspended in saline (1:10 dilution) through the microcatheter until distal stasis was achieved. Post-embolization DSA and cone beam CT (CBCT) were performed to confirm the embolization success. The microcatheter was repositioned before embolizing each arterial branch. One to three fundal arteries were embolized (Table 1, Figure 1). Control animals received 0.5 ml saline.

After BAE, a non-contrast CBCT was performed to confirm XEMs distribution. All catheters and sheaths were removed, and manual compression was applied to the femoral artery until hemostasis was achieved. Non-contrast CBCTs in anesthetized XEM-treated pigs were obtained weekly to determine the persistence of XEMs.

### In Vivo XEMs Radiopacity

To assess the persistence of XEMs *in vivo*, the radiopacities of XEMs (in Hounsfield unit, HU) were determined from CBCT images of the embolized stomach acquired one to four weeks after embolization. Circular region of interests were placed in regions of the stomach demonstrating XEMs and in the vertebral bodies of the spine to measure average signal intensity using vendor software (Syngo workstation, Siemens).

### Follow Up Examination

Following the procedure, individually housed pigs were fed their normal diet (Teklad Miniswine Diet 8753, Harlan Laboratories) twice a day. The pigs were weighed before the BAE procedure and every week thereafter, and fasting whole blood was collected from the jugular vein for hormone assessment. Total plasma ghrelin and glucagon-like peptide 1 (GLP-1) concentrations were assayed using a radioimmunoassay, and peptide YY (PYY) concentrations were assayed using an ELISA kit (Phoenix Pharmaceuticals, Burlingame, CA), as described previously (10).

Endoscopy of the stomach was performed one week after embolization to assess the effect of XEMs on stomach mucosa with a standard adult gastroscope (Pentax, Denver, CO). On the final imaging day, femoral arterial access was obtained as described above, and CBCT images and DSA of the gastric arteries were acquired. All pigs were then euthanized, and tissue was harvested for histological analysis.

### Gross Pathology

The excised distal esophagus, proximal duodenum, and stomach were opened along the greater curvature, pinned flat, photographed, and fixed with 10% formalin. The gastric mucosa was examined for evidence of mucosal ulceration, inflammation, or injury. CBCT images (Zeego, Siemens) were acquired on fixed stomachs to visualize the XEM locations. Tissue blocks from representative parts of the gastric fundus, body, antrum, and duodenum were taken from all pigs in approximately the same locations for histological analysis and toxicity assessment.

### Histological Analysis

Hematoxylin and eosin stained, 6-μm-thick slides were examined microscopically for mucosal integrity and the presence of microspheres. Adjacent sections were used for immunohistochemical detection of ghrelin- and gastrin-expressing cells using the primary mouse anti-ghrelin and mouse anti-gastrin antibodies (1:5,000, Millipore, Billerica, MA), respectively. Images were captured at 200× magnification using an upright microscope (Eclipse Ti, Nikon Instruments Inc., Melville, NY) and analyzed using NIS-Elements Basic Research, version 4.12, imaging software (Nikon Instruments Inc.). Ghrelin and gastrin immunoreactive cell numbers were counted and expressed as the mean number of positive cells per 200× high-power field.

For BAE animals, rhodizonate staining to identify barium particles was also performed to detect XEMs in tissue slices. To assess the degree of fibrosis, trichrome-stained sections

from gastric fundus were digitally scanned (Aperio, Leica Biosystems, Vista, CA) and analyzed using NIS-Elements Basic Research imaging software.

### Statistical Analysis

Data are presented as means ± standard deviation. Continuous data (e.g., weight, hormone levels) were analyzed using a cross-section time series regression analysis. Ordinal data (e.g., ghrelin- and gastric-expressing cell densities) were analyzed using a Wilcoxon rank sum test. P values less than 0.05 were considered statistically significant. Statistical analysis was performed using Stata (version 11, Stata Corp LP, College Station, TX).

## Results:

### Bariatric Arterial Embolization with XEMs

XEMs with mean diameter of 48.9 μm were synthesized. The endotoxin levels in XEMs prior to administration were negligible (< 2.50 endotoxin units/ml).

BAE was successfully performed in all animals. Targeted delivery of XEMs to the gastric fundus was achieved with direct visualization of XEMs during delivery on X-ray and CBCT, as well as during weekly follow-up on CBCT for up to four weeks (Figure 2A–D). The radiopacity of XEMs persisted for at least 4 weeks (165.4 ± 77 HU at one week vs. 158.5 ± 84 HU at four weeks) (Figure 2E). No visible reflux of delivered XEMs was noted during embolization.

NTE was observed in one of six experimental animals (Figure 2F). In this animal (GACE012), XEMs were visible by CBCT primarily in the left lobe of the liver, and there were a few XEMs delivered to the gastric body and antrum.

### Weight and Hormonal Changes

Weight declined in BAE animals at one week compared to weight gain in control animals (BAE: −1.43% ± 3.68; sham: 4.4% ± 2.8, P = 0.03), and weight gain remained significantly impaired at four weeks (14.3 %± 6.9 vs. 20.9 % ± 2 2, P < 0.01, Figure 3). The suppression of weight gain in BAE pigs was aligned with decreased serum ghrelin levels (BAE vs. control at 4 weeks: 1226 ± 523 pg/mL vs. 1706 ± 143 pg/mL, P < 0.001) (Figure 4A). While mean GLP-1 levels were increased in BAE animals as compared to control animals (BAE vs. control at 4 weeks: 9.9 ± 9.9 pM vs. 6.0 ± 2.3 pM, Figure 4B), this difference did not reach statistical significance (P = 0.47). In addition, there was no significant change in total plasma PYY levels between BAE and control animals (597.9 ± 132.0 pg/mL vs. 664.7 ± 117.5 pg/mL, P = 0.46) (Figure 4C).

### Gastric Ulceration

Endoscopy examination showed a mild, healing gastric ulcer at one-week post embolization in one XEM-treated pig (GACE009), who was embolized in all three major fundal arteries, and none of the control pigs. Gastritis was absent in all animals.

Gross examination of the pig stomachs revealed evidence of ulceration only in the XEM-treated pig that showed ulceration on endoscopy. This ulcer was completely healed at 4 weeks post-embolization. Normal gastric mucosa was noted in all sham animals. All other dissected organs, including heart, liver, lung, kidney, and pancreas, appeared grossly normal in both BAE and control animals.

### Histopathological Analysis

XEMs were identified in representative tissue blocks from all BAE animals by CBCT (Figure 5A), and the presence of XEMs was further confirmed to be restricted mainly in the fundal tissue of BAE animals by rhodizonate staining (Figure 5B). In one BAE pig, XEMs were also found in non-target gastric body and antrum, which agreed with the findings from CBCT images during XEM delivery. Trichrome staining showed well preserved gastric mucosa in both BAE and control animals (Figure 6A, 6B). However, much denser fibrotic infiltrates extending from submucosa to mucosa region was noted in all BAE animals (13.8 ± 4.5% vs 8.7 ± 2.2%, $P < 0.0001$, Figure 6).

The ghrelin immunoreactive mean cell counts were significantly lower in the gastric fundus (17.7 ± 10.5 vs 36.8 ± 10.7, $P < 0.00001$) and antrum (24.2 ± 9.4 vs 46.3 ± 18.3, $P < 0.0001$) of BAE pigs as compared to those of control pigs, but were similar in the duodenum (10.0 ± 5.1 vs 12.4 ± 3.0, $P = 0.16$) (Figure 7). Gastrin-producing cell counts in gastric antrum were markedly lower in BAE pigs relative to control pigs (98.5 ± 23 vs.127 ± 35, $P < 0.02$) (Figure 8).

## Discussion:

In this study, the safety and efficacy of BAE with custom-made, X-ray-visible, small sized, embolic microspheres and an anti-reflux catheter was demonstrated in a large swine model. The SureFire MT is a 3-French infusion catheter composed of a unique valve with a microfilter coating that enables forward flow, yet dynamically prevents retrograde flow during infusions. When combined with XEMs, the anti-reflux catheter facilitated precise targeting of the complex fundal arteries during BAE using CBCT guidance. The ability to directly visualize XEMs during and after delivery in three dimensions allowed the confirmation of target fundal embolization, the documentation of nontarget embolization, if present, and longitudinal examination of the persistence of XEMs, as well as the correlation of ulceration with XEMs distribution to ensure safe, targeted embolization of the fundal region of the stomach, where the majority of appetite-stimulating hormone, ghrelin, is produced (18, 19). Analogous to bariatric surgery, BAE targeting the fundus significantly affected weight gain and appetite-regulating gut hormones associated with obesity. In particular, both systemic and fundal ghrelin productions were significantly muted.

Although percutaneous transarterial embolization has been performed routinely by interventional radiologists for treating upper gastrointestinal artery bleeding (20, 21), the concept of BAE as a minimally invasive means to treat obesity is relatively new (22). The pioneering study performed by Arepally *et al.* demonstrated the feasibility and effectiveness of gastric arterial embolization in a swine model using liquid sclerosant, sodium morrhuate (10, 22). Although effective, the precise delivery of sodium morrhuate to target sites is

difficult and results in a high morbidity, e.g., tissue necrosis in the embolized stomachs (10, 22). Moreover, the 2D imaging techniques (i.e., ultrasonography and DSA) used in these early studies were inadequate to precisely map the complex vascular anatomy to distinguish vessels supplying the fundus versus other parts of the stomach or adjacent organs due to the lack of dimensional perspective offered by CBCT. This may have contributed to NTE which, in turn, leads to additional gastric ulceration away from the embolized areas.

Subsequent studies primarily have employed particle embolics to overcome the issues associated with liquid embolics (9, 11, 12, 15, 23, 24). To mimic the distal penetration properties of liquid embolics, Paxton *et al.* used commercially available, calibrated 40-μm particles for BAE in growing swine and demonstrated significantly impaired weight gain and reduced serum and fundal ghrelin levels in embolized animals (11, 13). However, in this study, half of the embolized pigs developed gastric ulcerations distant from the embolized fundus, suggesting, but not proving, that NTE might have occurred. Nevertheless, this study did demonstrate that smaller size particle embolics were able to achieve a similar embolization effect as liquid embolics with fewer adverse events. Since smaller size embolics tend to lodge more distally in the vasculature (25), this may increase the risk of gastric ulceration. In response, larger size embolics have been studied with mixed results (9, 12, 15). In one study, BAE was performed with either 150–250 μm or 50–150 μm non-spherical, polyvinyl alcohol particles (15). Unexpectedly, the study showed transient serum ghrelin reduction with similarly high rates of gastric ulcerations. In another study, Fu *et al.* compared the embolization effect of 100–300 μm and 300–500 μm trisacryl gelatin embolics in a relatively long 16-week study period and found only100–300 μm embolics were effective in suppressing weight gain and fundal ghrelin expression (9). However, 100–300 μm embolics were also associated with high risk of gastric ulcerations (100%). Because these embolic particles were radiolucent, neither of these studies could assess the full extent of NTE other than by post mortem evaluation (11, 13). In fact, no other BAE study to date has been able to accurately document either on- or off-target embolic distribution or microsphere persistence *in vivo*.

In contrast, the X-ray imaging visibility of XEMs, as demonstrated in this study, enabled the determination of whether NTE occurred during the embolization procedure which may help reduce clinically significant NTE. The single pig with NTE had a right gastric artery with a short take-off from the hepatic artery, leading to NTE in the liver. Additionally, pressurization by the Surefire catheter could push microspheres delivered to the left gastroepiploic artery (LGEA), which feeds the fundus, into right gastroepiploic artery with which the LGEA anastomoses, resulting in NTE in the body and antrum. In a clinical scenario, it is reasonable to assume that NTE could be avoided using a similar radiopaque embolic. When combined with CBCT and anti-reflux catheters, XEMs could be targeted to fundal vasculature of submucosa with better precision, which may lower the incidence of ulceration (17%). This is a significant improvement when compared to earlier studies where 40–100% ulceration rates have been reported irrespective of the embolic sizes (11, 13, 15). This reduced ulceration could also be due to the combination of the size, compressibility, and quantity of XEMs administered. The small size XEMs may provide more distal penetration and earlier stasis, thus preserving more proximal vasculature supplying the entire expanse of musculature to the stomach. In addition, low volume of XEMs could be used as

compared to BAE with other bland embolics (9), which may have contributed to less damage to the gastric mucosa. In this study, ulceration was noted in single animal who received embolization in all three major fundal arteries, suggesting ischemia due to “over”-embolization was the likely culprit. The decreased weight gain in XEM-treated pigs was aligned with markedly reduced systemic and fundal ghrelin levels. This agrees with previous studies using similar size embolics (11, 13). The persistence of the radiopacity of XEMs over time could enable CT imaging to address the need for and timing of repeat embolization in a clinical population.

This study has several limitations that require further studies to determine long-term XEM stability and efficacy, and the effect of embolization coverage (single vs. multi-vessel embolization) on outcomes. As a proof of concept study for imaging-visible embolics, $BaSO_4$ was chosen as a contrast agent as it is widely used in clinic for gastrointestinal (GI) tract studies and has been previously shown in larger alginate embolics to provide a high radiopacity with excellent biocompatibility (26). In this study, $BaSO_4$ was uniformly embedded within alginate matrix, which was stable for over a 6-month testing period. In addition, the total load of $BaSO_4$ in the embolic microspheres per animal was < 7.4 mg, which is small compared to GI leaks. Given the poor solubility of $BaSO_4$, potential elusion of the barium from XEMs is minimal, but its impact on long-term biocompatibility and other complications can’t be foreseen. Nevertheless, the fibrosis in the stomach submucosa was generalized rather than localized to perivascular XEM locations. In addition, the lack of rhodizonate staining in the absence of XEMs or the presence of a foreign body reaction suggests that free $BaSO_4$ was not the major driver of fibrosis. Thus, it is likely that embolic ischemia rather than $BaSO_4$ toxicity is the primary cause of fibrosis.

While the weight gain and systemic ghrelin levels were consistently suppressed in XEM-embolized pigs for up to four weeks post procedure, early clinical studies using bland large size particle embolics have demonstrated that the weight gain/loss and ghrelin levels that were initially suppressed might return to baseline levels at later time points (1, 2), suggesting that future studies with longer-term evaluation of XEMs will be warranted. In addition, the sample size of the current study was relatively small, and a definitive conclusion regarding whether the embolization coverage affected the safety or efficacy of BAE or effects on other gastric hormones, such as PYY and GLP-1, could not be reached. Nevertheless, BAE with XEMs and an anti-reflux catheter reduced weight gain and ghrelin production in the short term in growing pigs.

In conclusion, BAE with imaging-visible embolic microspheres enabled direct visualization of the embolic during and after the embolization procedures. When combined with an anti-reflex catheter, BAE with XEMs ensured precise delivery of XEMs to minimize NTE, thus enhancing the safety of BAE. The significant suppression of weight gain and systemic and fundal ghrelin levels suggests that BAE with XEMs may provide a viable interventional approach for treatment of the obese patient.

## Acknowledgments:

The work is supported by NIH R21/R33 HL089029, NIH R01 EB017615, AHA 16SDG30500010, Maryland Stem Cell Research Fund 2011-MDSCRFII-0043, and Siemens Healthcare.

## References:


1. Bai ZB, Qin YL, Deng G, et al. Bariatric Embolization of the Left Gastric Arteries for the Treatment of Obesity: 9-Month Data in 5 Patients. Obes Surg. 2018;28(4):907–15. [PubMed: 29063494]
2. Weiss CR, Abiola GO, Fischman AM, et al. Bariatric Embolization of Arteries for the Treatment of Obesity (BEAT Obesity) Trial: Results at 1 Year. Radiology. 2019;291(3):792–800. [PubMed: 30938624]
3. Weiss CR, Akinwande O, Paudel K, et al. Clinical Safety of Bariatric Arterial Embolization: Preliminary Results of the BEAT Obesity Trial. Radiology. 2017;283(2):598–608. [PubMed: 28195823]
4. Syed MI, Morar K, Shaikh A, et al. Gastric Artery Embolization Trial for the Lessening of Appetite Nonsurgically (GET LEAN): Six-Month Preliminary Data. J Vasc Interv Radiol. 2016;27(10):1502–8. [PubMed: 27567998]
5. Kipshidze N, Archvadze A, Bertog S, et al. Endovascular Bariatrics: First in Humans Study of Gastric Artery Embolization for Weight Loss. JACC Cardiovasc Interv. 2015;8(12):1641–4. [PubMed: 26493259]
6. Zaitoun MMA, Basha MAA, Hassan F, et al. Left Gastric Artery Embolization in Obese, Prediabetic Patients: A Pilot Study. J Vasc Interv Radiol. 2019;30(6):790–6. [PubMed: 31040059]
7. Kojima M, Hosoda H, Date Y, et al. Ghrelin is a growth-hormone-releasing acylated peptide from stomach. Nature. 1999;402(6762):656–60. [PubMed: 10604470]
8. Gunn AJ, Oklu R. A preliminary observation of weight loss following left gastric artery embolization in humans. J Obes. 2014;2014:185349. [PubMed: 25349724]
9. Fu Y, Weiss CR, Paudel K, et al. Bariatric Arterial Embolization: Effect of Microsphere Size on the Suppression of Fundal Ghrelin Expression and Weight Change in a Swine Model. Radiology. 2018;289(1):83–9. [PubMed: 29989526]
10. Arepally A, Barnett BP, Patel TH, et al. Catheter-directed gastric artery chemical embolization suppresses systemic ghrelin levels in porcine model. Radiology. 2008;249(1):127–33. [PubMed: 18796671]
11. Paxton BE, Kim CY, Alley CL, et al. Bariatric embolization for suppression of the hunger hormone ghrelin in a porcine model. Radiology. 2013;266(2):471–9. [PubMed: 23204538]
12. Bawudun D, Xing Y, Liu WY, et al. Ghrelin suppression and fat loss after left gastric artery embolization in canine model. Cardiovasc Intervent Radiol. 2012;35(6):1460–6. [PubMed: 22367009]
13. Paxton BE, Alley CL, Crow JH, et al. Histopathologic and immunohistochemical sequelae of bariatric embolization in a porcine model. J Vasc Interv Radiol. 2014;25(3):455–61. [PubMed: 24462005]
14. Fu Y, Kraitchman DL. Rationale and Preclinical Data Supporting Bariatric Arterial Embolization. Tech Vasc Interv Radiol. 2020;23(1):100656. [PubMed: 32192641]
15. Kim JM, Kim MD, Han K, et al. Bariatric Arterial Embolization with Non-spherical Polyvinyl Alcohol Particles for Ghrelin Suppression in a Swine Model. Cardiovasc Intervent Radiol. 2017;40(5):744–9. [PubMed: 28184958]
16. Paxton BE, Arepally A, Alley CL, Kim CY. Bariatric Embolization: Pilot Study on the Impact of Gastroprotective Agents and Arterial Distribution on Ulceration Risk and Efficacy in a Porcine Model. J Vasc Interv Radiol. 2016;27(12):1923–8. [PubMed: 27717647]
17. Unger MA, Chou HP, Thorsen T, et al. Monolithic microfabricated valves and pumps by multilayer soft lithography. Science. 2000;288(5463):113–6. [PubMed: 10753110]
18. Tanaka-Shintani M, Watanabe M. Distribution of ghrelin-immunoreactive cells in human gastric mucosa: comparison with that of parietal cells. J Gastroenterol. 2005;40(4):345–9. [PubMed: 15870970]
19. Vitari F, Di Giancamillo A, Deponti D, et al. Distribution of ghrelin-producing cells in the gastrointestinal tract of pigs at different ages. Vet Res Commun. 2012;36(1):71–80. [PubMed: 22281862]

20. Beggs AD, Dilworth MP, Powell SL, et al. A systematic review of transarterial embolization versus emergency surgery in treatment of major nonvariceal upper gastrointestinal bleeding. Clinical and Experimental Gastroenterology. 2014;7:93–104. [PubMed: 24790465]

21. Lee CW, Liu KL, Wang HP, et al. Transcatheter arterial embolization of acute upper gastrointestinal tract bleeding with N-butyl-2-cyanoacrylate. J Vasc Interv Radiol. 2007;18(2):209–16. [PubMed: 17327553]

22. Arepally A, Barnett BP, Montgomery E, Patel TH. Catheter-directed gastric artery chemical embolization for modulation of systemic ghrelin levels in a porcine model: initial experience. Radiology. 2007;244(1):138–43. [PubMed: 17581899]

23. Diana M, Pop R, Beaujeux R, et al. Embolization of arterial gastric supply in obesity (EMBARGO): an endovascular approach in the management of morbid obesity. proof of the concept in the porcine model. Obes Surg. 2015;25(3):550–8. [PubMed: 25511751]

24. Pasciak AS, Bourgeois AC, Paxton BE, et al. Bariatric Radioembolization: A Pilot Study on Technical Feasibility and Safety in a Porcine Model. J Vasc Interv Radiol. 2016;27(10):1509–17. [PubMed: 27492867]

25. Stampfl S, Bellemann N, Stampfl U, et al. Arterial distribution characteristics of Embozene particles and comparison with other spherical embolic agents in the porcine acute embolization model. J Vasc Interv Radiol. 2009;20(12):1597–607. [PubMed: 19944985]

26. Fu Y, Azene N, Ehtiati T, et al. Fused X-ray and MR imaging guidance of intrapericardial delivery of microencapsulated human mesenchymal stem cells in immunocompetent swine. Radiology. 2014;272(2):427–37. [PubMed: 24749713]

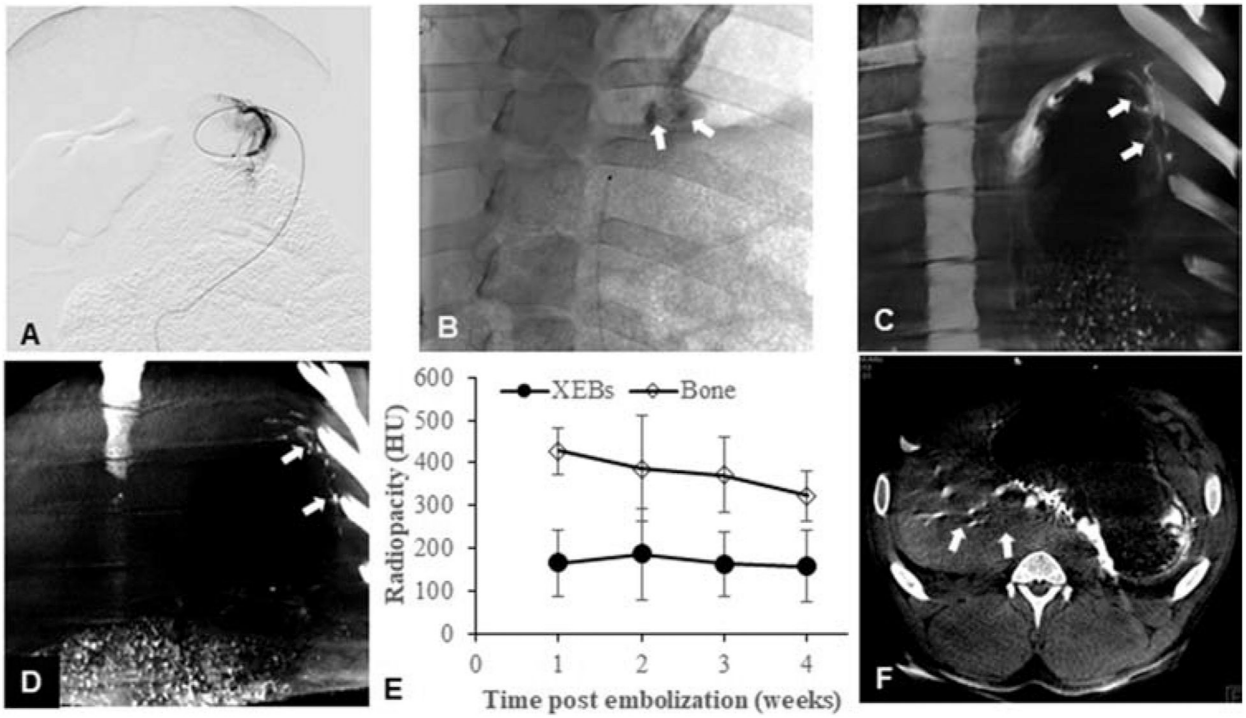


**Figure 1.**

(A) Pre-embolization celiac digital subtraction angiogram (DSA) of the stomach shows the right gastric artery (black arrow), left gastric artery (*), and left gastroepiploic artery (white arrows) that supply the gastric fundus. (B) Post-embolization DSA of the same animal after superselective embolization of the right gastric artery and the left gastroepiploic artery confirms the stasis of blood flow.

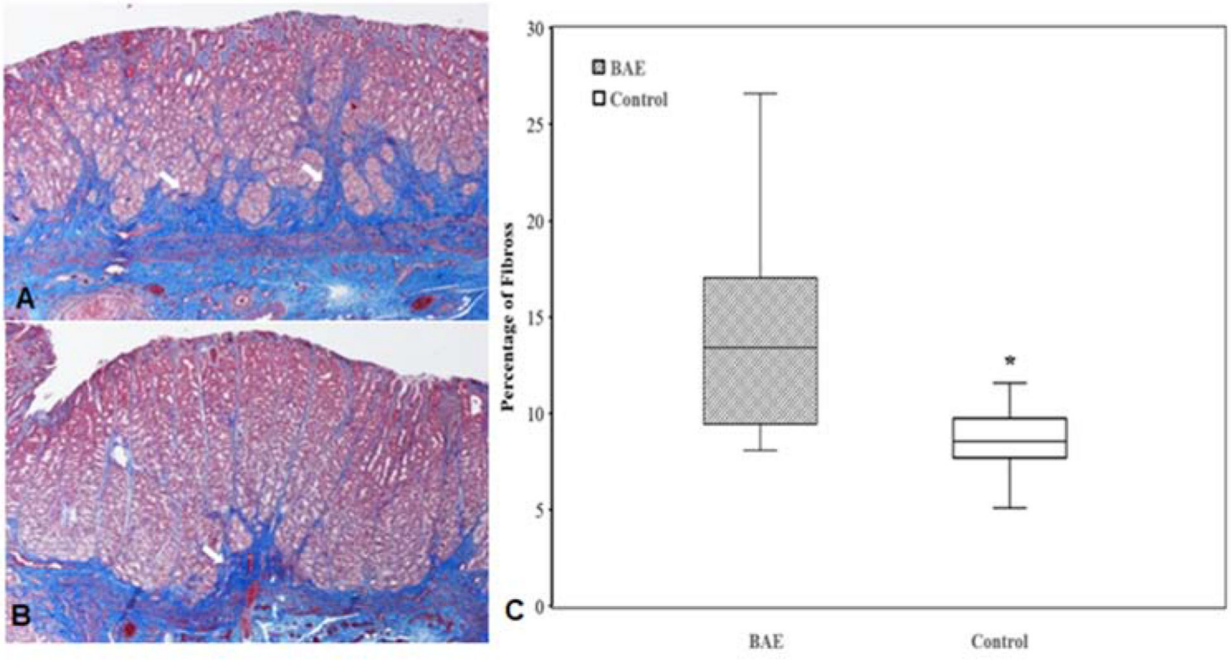


**Figure 2.**

*In vivo* X-ray visibility of XEMs. (A) Sub-selective angiogram of left gastroepiploic artery shows the placement of the anti-reflux catheter. (B) Single shot X-ray image during right gastric artery embolization shows the visibility of XEMs during delivery (arrows). (C, D) Coronal view of CBCT images of the stomach immediately (C) and 4 weeks (D) after embolization shows persistent visualization of XEMs in the stomach (arrows). (E) Graph of CT numbers for XEMs and bone demonstrates that *in vivo* radiopacity of XEMs remains unchanged over time and was similar to that of bone (P = 0.9). (F) Axial view of CBCT image of the stomach after BAE reveals non-target embolization mostly to the liver (arrows).

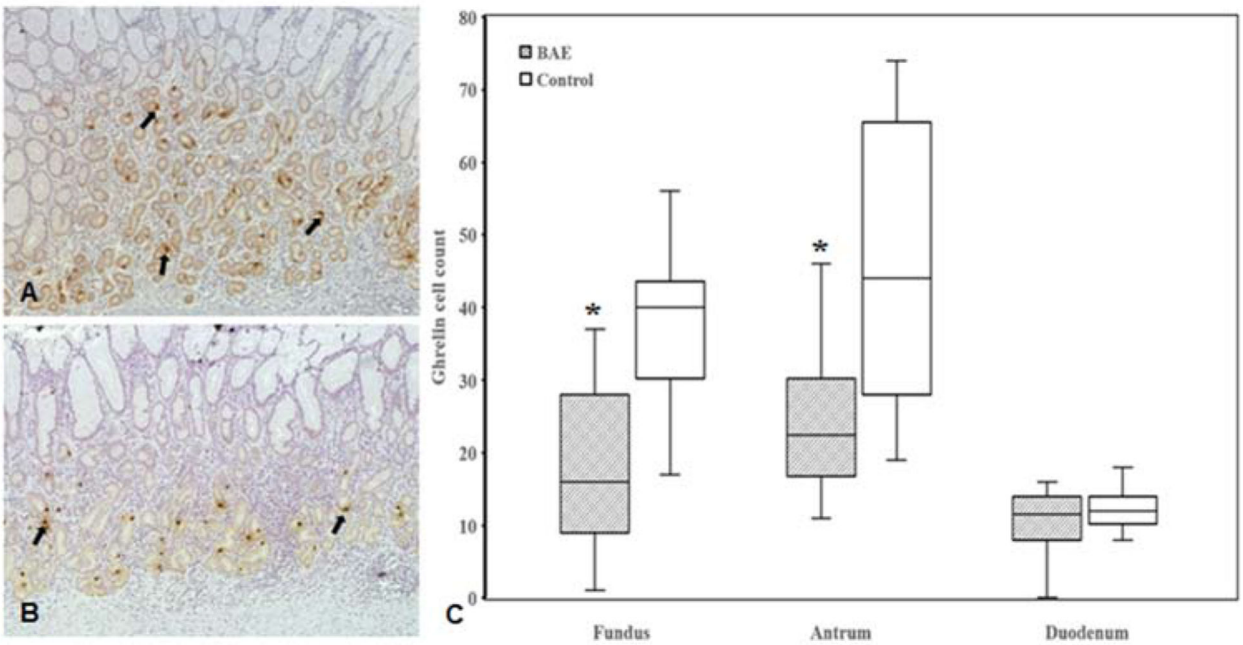


**Figure 3.**

Mean percentage weight change from baseline after bariatric arterial embolization (BAE) shows initial weight decline in embolized animals one week after BAE and suppressed weight gain over 4 weeks relative to controls (week 1: $P = 0.03$, week 2 and week 4: $P < 0.01$).

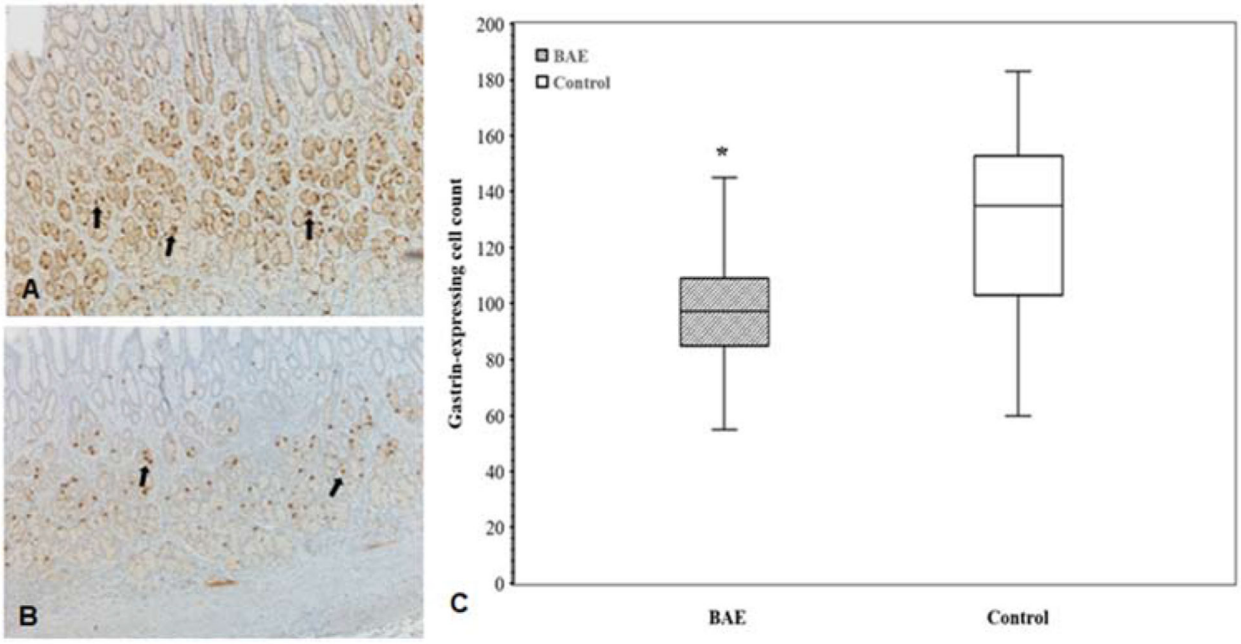


**Figure 4.**

Weekly plasma hormone levels over the 4-week study. (A) Mean plasma ghrelin levels were significantly lower in BAE animals as compared to those of control ($P < 0.001$). (B) GLP-1 levels were consistently higher in embolized animals than in controls. Yet, no significant difference was noted. (C) Plasma PYY levels were similar between BAE animals and controls.

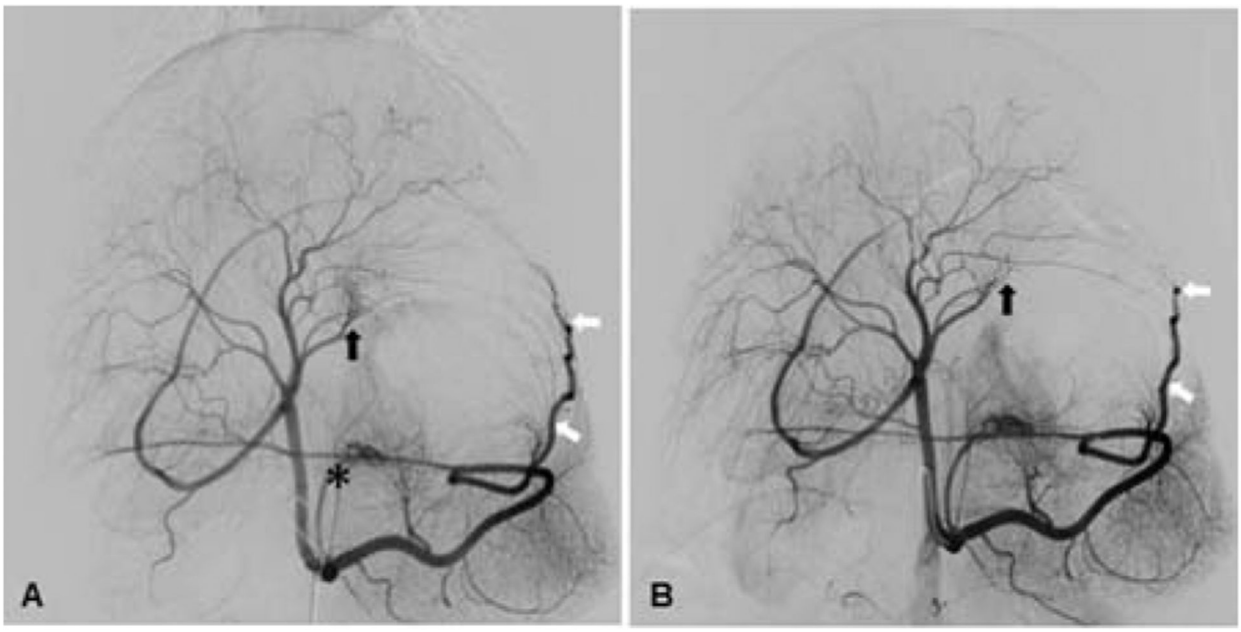


**Figure 5.**

Postmortem identification of XEMs. (A) XEMs were identified in representative tissue blocks from BAE animals by CBCT (arrows). (B) Rhodizonate staining of the tissue sections from BAE animals confirmed the presence of XEMs (arrows).

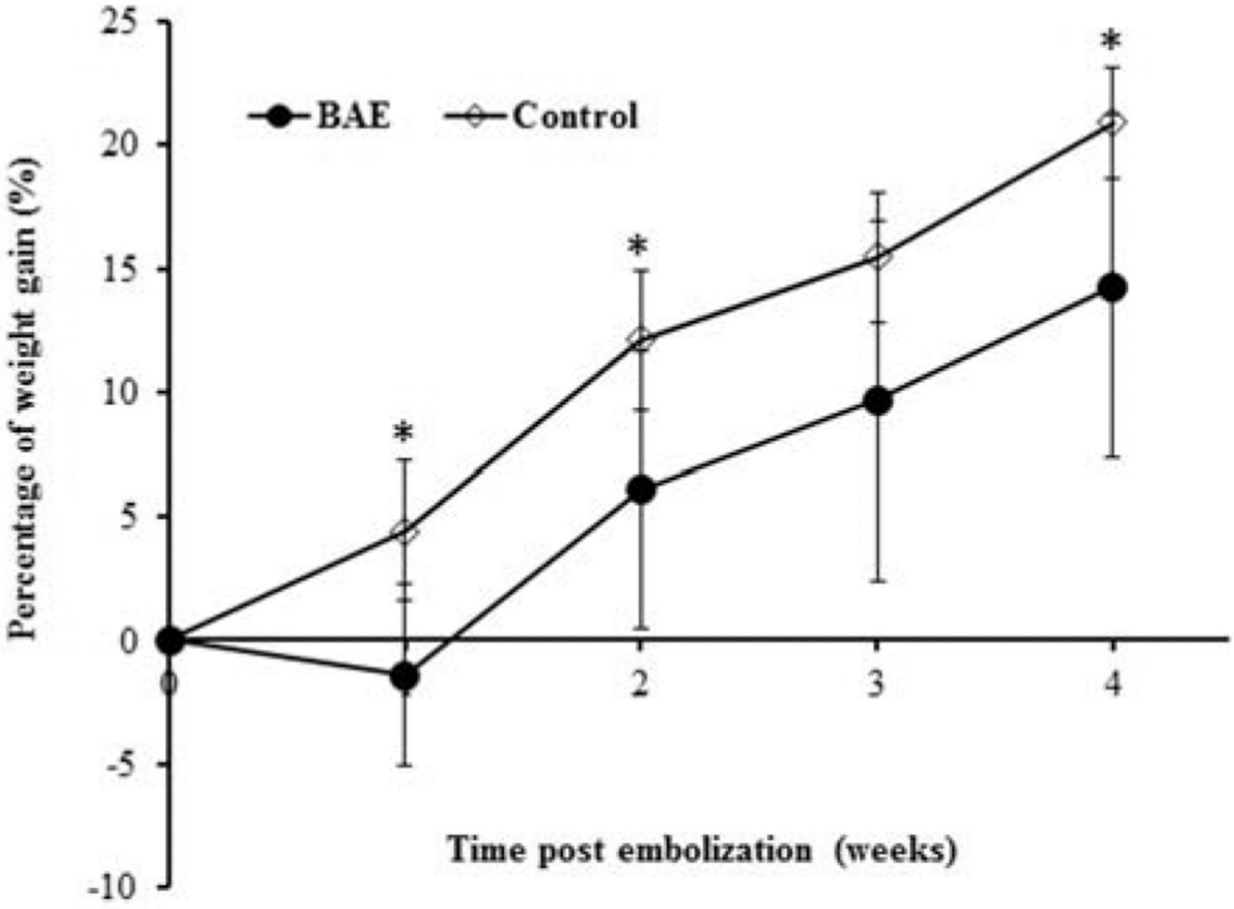


**Figure 6.**

Trichrome staining of the gastric fundus shows dense fibrotic infiltrates (arrows) extending from submucosa to mucosa region in BAE animals (A) relative to controls (B). (C) Box plot of percentage fibrosis in the gastric fundal mucosa reveals prominent fibrosis in BAE animals compared with control animals ($P < 0.0001$).

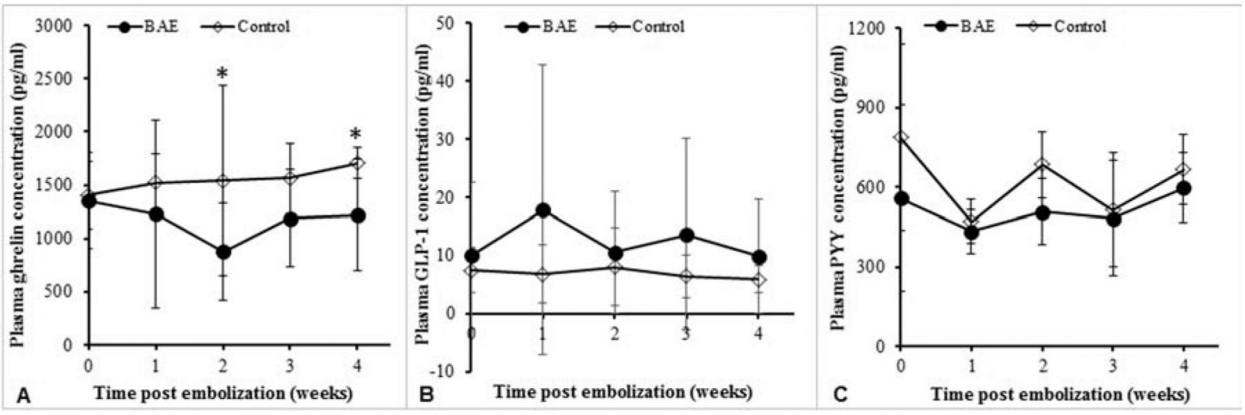


**Figure 7.**

(A, B) Representative images of immunohistochemical staining of ghrelin-expressing cells (arrows) in the gastric fundus of embolized animals (A) and controls (B). (C) Box plot of ghrelin-expressing cell counts shows statistically significant reduction of ghrelin-expressing cells in the gastric fundus ($P < 0.00001$)and body ($P < 0.0001$) of the embolized animals relative to controls without compensatory upregulation in the duodenum ($P = 0.16$).

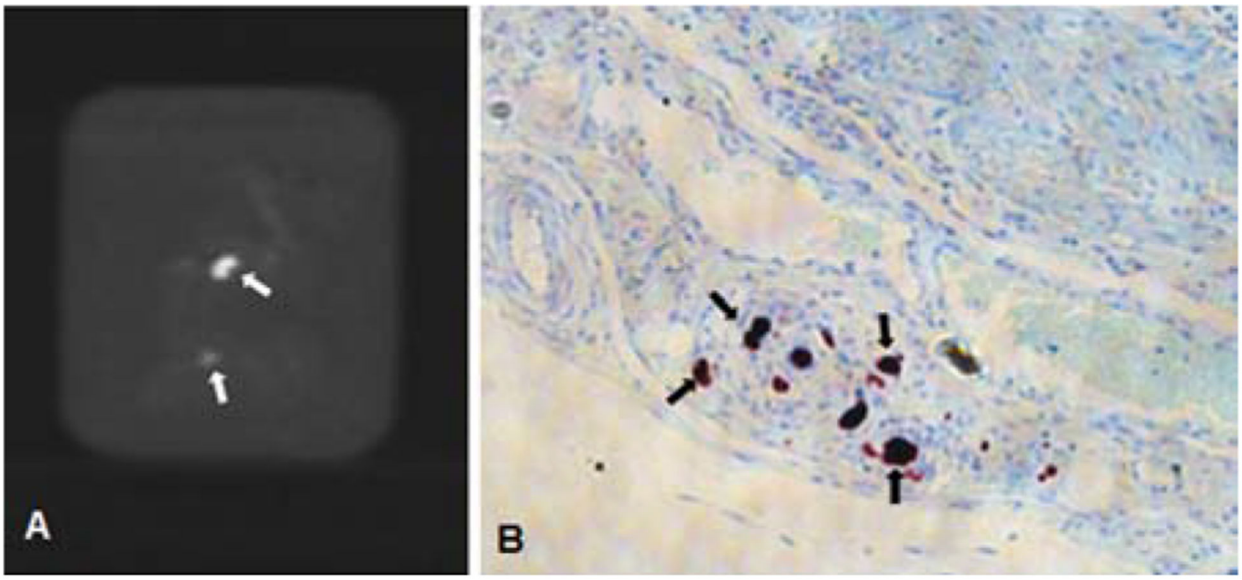


**Figure 8.**

(A, B) Representative images of immunohistochemical staining of gastrin-expressing cells (arrows) in the gastric antrum of embolized animals (A) and controls (B). (C) Box plot of gastrin-expressing cell counts shows statistically significant reduction of gastrin-expressing cells in the gastric antrum ($P < 0.02$) of embolized animals as compared to controls.

**Table 1.**

Animal characteristics and gastric arteries embolized

| Animal ID | Initial Weight (lb) | Arteries Embolized | | |
|---|---|---|---|---|
| | | Left Gastroepiploic Artery (LGEA) | Left Gastric Artery (LGA) | Right Gastric Artery (RGA) |
| GACE005 | 80.0 | + | + | − |
| GACE006 | 59.7 | + | + | − |
| GACE007 | 51.3 | + | + | − |
| GACE008 | 69.7 | − | − | − |
| GACE009 | 54.0 | + | + | + |
| GACE010 | 69.7 | + | − | − |
| GACE011 | 68.6 | − | − | − |
| GACE012 | 60.0 | + | − | − |
| GACE013 | 65.9 | − | − | − |
| GACE014 | 66.6 | − | − | − |